Multi-Path Transmission of Real-Time Remote Sensing Data via Heterogeneous LEO Inter-Satellite-Links

Binquan Guo[a,b,c], Zehui Xiong[c*], Dusit Niyato[d], Shiwen Mao[e], and Zhu Han[f]
[a]School of Telecommunication Engineering, Xidian University, Xi'an 71071, P. R. China
[b]Tianjin Artificial Intelligence Innovation Center (TAIIC), Tianjin 300457, P. R. China
[c]Pillar of ISTD, Singapore University of Technology and Design, 487372, Singapore
[d]College of Computing and Data Science, Nanyang Technological University, 639798, Singapore
[e]Department of Electrical and Computer Engineering, Auburn University, Auburn, AL 36849, USA
[f]Department of Electrical and Computer Engineering, University of Houston, Houston, TX 77004, USA
Email: bqguo@stu.xidian.edu.cn, zehui_xiong@sutd.edu.sg, dniyato@ntu.edu.sg,
smao@ieee.org, hanzhu22@gmail.com

2024 IEEE 21st International Conference on Mobile Ad-Hoc and Smart Systems (MASS) | 979-8-3503-6399-9/24/$31.00 ©2024 IEEE | DOI: 10.1109/MASS62177.2024.00021

***Abstract*—Real-time transmission of remote sensing data is critical for many applications. The rapid enhancement in sensing capabilities has posed challenges in sending large volumes of collected information to users on the ground in a timely manner. Deployed with inter-satellite links (ISLs), low-earth-orbit mega-constellations can facilitate the relay of remote sensing data to ground stations. However, due to scarce spectrum resources, increasing data throughput remains a challenge. Towards this, we explore multi-path transmission of real-time remote sensing data via heterogeneous ISLs, with the aim of maximizing data transmission throughput. We formulate the problem of multi-path transmission via heterogeneous ISLs as a linear programming problem, and find that its complexity is exacerbated when dealing with large-scale satellite networks. Therefore, we present an alternative approach using graph theory, transforming the problem into a classical maximum flow problem. This approach ensures optimal resolution of the original problem within polynomial time. Simulations conducted on the Gaofen and Starlink constellation demonstrate the performance benefits of our approach regarding both time complexity and throughput.**

***Index Terms*—Satellite networks, remote sensing, inter-satellite links, graph theory, multi-path transmission.**

I. Introduction

Remote sensing satellites observe Earth from orbit and transmit the sensed data to the ground for purposes such as disaster relief, environmental surveillance, weather forecasting, and emergency monitoring. Real-time transmission of remote sensing data is crucial for many important time-critical applications, particularly in scenarios like forest fire monitoring and emergency rescue in remote areas. However, most current remote sensing systems are limited to direct communication with ground stations. As a result, data from today's operational remote sensing satellites must wait in orbit for long periods until satellites pass over ground stations within their coverage for downloading. This store-carry-download approach significantly limits the applicability of remote sensing systems in many time-sensitive scenarios [1]. The surge in large-scale low-earth-orbit (LEO) satellite deployments has demonstrated the potential for low-latency transmission of remote sensing data via inter-satellite links (ISLs). By leveraging ISLs, remote sensing satellites beyond the coverage of ground stations can relay data through multiple LEO relay satellites [2]. Actually, ISLs have already been successfully demonstrated in satellite systems such as BeiDou [3] and Iridium [4]. They will also be deployed in the Starlink [5] (i.e., in its second step) and Hongyan [6] constellations to enhance real-time communication capabilities. According to [7], utilizing inter-satellite communication can reduce end-to-end delay to tens of milliseconds, highlighting its significant potential for supporting real-time transmission of remote sensing data.

Due to advancements in remote sensing capabilities, such as the transition from optical to multi/hyper-spectral imaging, the data volume of remote sensing systems has significantly increased. This enhancement has led to an enormous increase in sensed data, making the real-time transmission of this data from space to ground stations a challenging task. In 2014, it was reported that NASA's remote sensing system (i.e., EOSDIS) downloaded over one billion data files, amounting to 27.9 Terabytes per day [8]. By 2019, satellites such as MODIS, Landsat-7/8, and the Sentinel series had generated a cumulative data volume of 5 Petabytes [9]. Notably, when functioning at maximum capacity, a single Landsat-8 satellite is capable of producing up to 0.7 Terabytes of images each day [10]. However, the mobility of satellites leads to intermittent connections within satellite networks. The dynamic positions of LEO relay satellites result in no fixed communication path between remote sensing satellites and ground stations. This intermittency significantly impacts the data throughput for real-time remote sensing data transmission. Because satellites are continuously moving and have limited communication windows with ground stations, shortest path-based methods such as [11]–[13] often fail to satisfy the bandwidth demands of extensive remote sensing data. Consequently, even though ISLs can reduce end-to-end latency, they still face significant challenges in meeting high-throughput demands due to their

2155-6814/24/$31.00 ©2024 IEEE
DOI 10.1109/MASS62177.2024.00021

limited capacity.

Indeed, current satellite networks primarily utilize radio-frequency (RF) bands across a range of frequencies, encompassing L-band to Ka-band. Higher frequencies within these bands support higher data rates, which is essential for various satellite communication needs [14]. However, RF communication faces significant challenges such as limited spectrum availability, congestion, interference, and regulatory constraints. These issues hinder the ability to realize transmission of real-time remote sensing data at high data rates. To address these challenges, combining RF and Free Space Optical (FSO) communication technologies is considered a viable approach. FSO operates in unlicensed bands and offers broadband speeds up to several Gigabits per second, with minimal cost and power consumption [15]. This hybrid approach ensures continuous link availability by dynamically switching between RF and FSO based on environmental conditions. Moreover, by coordinating heterogeneous ISL resources in dynamic satellite networks, additional communication opportunities can be exploited. This coordination allows for the exploration of multiple-path transmission options [16], further enhancing the robustness and efficiency of satellite communications. The integration of RF and FSO technologies thus provides a more resilient and efficient data transmission framework, capable of supporting the growing demands for high-throughput and real-time remote sensing data transmission.

In this study, our objective is to explore the advantages of using a multi-path transmission scheme that exploits heterogeneous ISLs to improve throughput in remote sensing data transmission. Instinctively, increasing throughput involves leveraging more communication opportunities. However, the performance gain heavily depends on the design of efficient routing strategies. Previous studies have designed various routing methods to enhance data transmission performance in satellite networks for either delay-tolerant tasks [17]–[21] or real-time applications [22]–[25]. These methods primarily address link dynamics and bandwidth resource allocation but do not consider the scheduling of ISLs. Regarding ISL resource allocation in satellite networks, extensive research has been conducted to address constraints related to the number of transceivers [26]–[31]. However, these studies generally assume that satellite nodes are equipped with homogeneous transceivers and do not account for the cooperation of heterogeneous transceivers.

Towards this goal, we explore the multi-path transmission of real-time remote sensing data via heterogeneous ISLs, with the aim of maximizing data transmission throughput. We formulate the problem of multi-path transmission via heterogeneous ISLs as a linear programming problem. However, solving this problem in large-scale satellite networks is highly complex. To overcome this, we develop an alternative graph-based method that transforms the problem into a classical maximum flow one, providing an efficient solution within polynomial time. Simulations conducted on the Gaofen and Starlink constellation demonstrate the performance benefits of our approach regarding both time complexity and throughput.

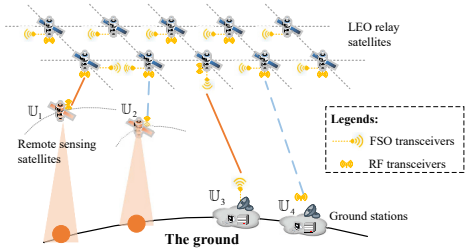

Fig. 1. The scenario of satellite networks with heterogeneous LEO ISLs.

II. System Model

A. Satellite Network Model

We consider a satellite network comprising remote sensing satellites, relay satellites, and ground stations. The relay satellites are represented by the set $\mathcal{S} = \{\mathbb{S}_1, ..., \mathbb{S}_P\}$. The remote sensing satellites and ground stations, referred to as user equipments (UEs), are gathered into the set $\mathcal{U} = \{\mathbb{U}_1, ..., \mathbb{U}_K\}$. Here, P denotes the size of set $\mathcal{S}$, while K denotes the size of set $\mathcal{U}$. Each UE can be either a remote sensing satellite or a ground station, requiring real-time data transmission or reception. Each satellite or UE is equipped with one or multiple types of transceivers (e.g., RF and FSO), which are heterogeneous and capable of mixed-mode data transmission across different hops. Additionally, the satellite network supports ISLs, which are intermittent and predictable based on the periodical movement of the satellites. This combination of RF and FSO allows for data transmission, utilizing RF communication in one hop and FSO communication in another, optimizing performance based on environmental conditions and link characteristics.

The collection of heterogeneous transceiver types employed in the satellite network is represented by $\mathcal{F} = \{f_1, f_2, ..., f_N\}$, where N signifies the number of distinct transceiver types. We assume that various transceivers, operating in different RF bands, or using FSO, are deployed across different satellites or UEs within the satellite network. Unlike the homogeneous transceiver assumption in [26], each satellite can be equipped with one or multiple types of heterogeneous transceivers. Furthermore, various switching methodologies can be adopted, including soft-switching and hard-switching. Soft-switching allows for the simultaneous activation of multiple links, whereas hard-switching restricts the activation to only one link at a time. Utilizing these techniques, satellites can effectively coordinate to schedule different transceivers.

To represent the transceivers equipped on different satellites, we define a binary vector $\mathcal{W}_{\mathbb{S}_i} = \{w_{\mathbb{S}_i}^{f_l} | f_l \in \mathcal{F}\}$ for each satellite $\mathbb{S}i$. In this vector, $w_{\mathbb{S}_i}^{f_l} = 1$ indicates that satellite $\mathbb{S}_i$ is equipped with a transceiver of type f_l, while $w_{\mathbb{S}_i}^{f_l} = 0$ indicates the absence of a transceiver of type f_l on that satellite. Similarly, UE can also be equipped with various types of transceivers. We define the binary vector $\mathcal{W}_{\mathbb{U}_i} = \{w_{\mathbb{U}_i}^{f_l} | f_l \in \mathcal{F}\}$ for each UE $\mathbb{U}_i$. Here, $w_{\mathbb{U}_i}^{f_l} = 1$ means that UE $\mathbb{U}_i$ is equipped with a transceiver of type f_l, and $w_{\mathbb{U}_i}^{f_l} = 0$ indicates that type f_l is not available on that UE.

B. Real-Time Remote Sensing Data Transmission Application Model

During a time period $\mathcal{T}$, we define a real-time remote sensing data transmission application $\mathcal{A} = \{\mathbb{U}_s, \mathbb{U}_d\}$ that requires data transmission from a source UE $\mathbb{U}_s$ to a destination UE $\mathbb{U}_d$, with the aim of maximizing throughput (Unit: Mbps). Here, the source UE is a remote sensing satellite, while the destination UE is a ground station. Each UE or satellite may be equipped with one or multiple types of transceivers. Therefore, we assume that each real-time remote sensing data transmission application necessitates a multi-path transmission scheme. Each path can consist of multiple hops, with the constraint that the nodes at either end of a hop must have the same type of transceiver. Thus, a multi-path transmission scheme for $\mathcal{A}$ ensures that each link in the selected paths comprises nodes with identical type of transceivers, while different links within each path may utilize heterogeneous transceivers for data transmission. Since the application operates in real time, the duration and the data size of the application are unknown.

An example. Consider a scenario involving large-scale satellite networks equipped with heterogeneous ISLs, as depicted in Figure 1. In this scenario, there exist two distinct transceiver types, i.e., RF and FSO. Each transceiver can only communicate with others of the same type within its communication range. Each application consists of a node pair representing the source and sink UEs. For efficient data transmission between the source UE and the sink UE, a multi-path routing scheme that maximizes throughput needs to be developed. This multi-path transmission approach maximizes the utilization of communication opportunities while ensuring that each link within every selected path adheres to the transceiver matching constraints. This guarantees the highest possible end-to-end transmission rates for real-time remote sensing data.

C. Time-Varying Graph Model

Due to the mobility of satellites and changes in transceiver resources, both the satellite network topology and link attributes are time-varying. To mitigate the impact of dynamic topology on satellite routing performance, a *time division mechanism* is employed to partition the given time period into multiple time slices. Each slice maintains a stable and static network topology snapshot. There are two primary time division mechanisms. One approach, introduced by [32], generates a new snapshot whenever an ISL is established or broken, with connectivity changes triggered by line-of-sight distance thresholds. The other approach, proposed by [33], uses equal time intervals for snapshots due to its practicality and straightforward management. For example, the Iridium constellation uses the latter approach with each snapshot lasting 2.5 minutes [34]. However, both approaches focus solely on node movement behaviors and do not consider transceiver resources, making them unsuitable for scenarios with heterogeneous transceivers.

To address this issue, we adopt an enhanced time division mechanism based on [35]. This revised procedure leverages the concept of the *contact plan* [11], defined as a list $\mathcal{Y}$ encompassing all topological changes of the satellite network and transceiver resources over the time horizon $\mathcal{T}$. The entries in this list, called *contacts*, are denoted as tuples $< t_s, t_e, \mathbb{O}_i, \mathbb{O}_j >$, indicating a communication opportunity from node $\mathbb{O}_i$ to node $\mathbb{O}_j$ with certain transceiver resources available during the time interval $[t_s, t_e]$. Despite the variability in communication opportunities and resource availability over time, they are stable within each time window. Consequently, the enhanced time division mechanism effectively manages the availability of heterogeneous transceiver resources.

Leveraging the enhanced time division mechanism, the time horizon $\mathcal{T} = [0, T]$ is partitioned into time windows of varying durations. Each time window, denoted by $\tau = [t_s, t_e]$, with $|\tau| = t_e - t_s$ representing the duration. We segment $\mathcal{T}$ into multiple time windows so that within each window τ, the availability of transceivers on nodes, as well as link connectivity and delays, remain constant.

Then, we utilize snapshot graphs to depict the evolving satellite network across discrete time windows. The snapshot graph for the time interval τ is denoted by $\mathcal{G}^\tau = (\mathcal{V}^\tau, \mathcal{L}^\tau)$. Here, $\mathcal{V}^\tau = \mathcal{S} \cup \mathcal{U}$ is the set of available LEO relay satellites and UEs, and $\mathcal{L}^\tau$ is the set of potential communication opportunities, encompassing both UE-satellite links (USLs) and ISLs within the time interval τ. Given the predictable and periodic nature of satellite movement, all communication opportunities can be known in advance.

For each node, whether a satellite or UE, $\mathbb{O}_i \in \mathcal{S} \cup \mathcal{U}$, we define the set $\mathcal{W}_{\mathbb{O}_i} = \{w^{f_1}_{\mathbb{O}_i}, w^{f_2}_{\mathbb{O}_i}, ..., w^{f_N}_{\mathbb{O}_i}\}$ to indicate the availability of each transceiver type, where $|\mathcal{W}_{\mathbb{O}_i}| = N$. A communication opportunity exists whenever a UE or satellite is within the coverage area of another satellite. Unlike previous works such as [26], which assume uniform data rates, our model considers that satellite antennas have different data rates for receiving and transmitting. The achievable transmission rate of node $\mathbb{O}_i$ using a type-f_l transceiver during a communication opportunity $(\mathbb{O}_i, \mathbb{O}_j)$ in the time window τ is represented by $r^\tau_{\mathbb{O}^{f_l}_i, \mathbb{O}_j}$, while the achievable receiving rate for node $\mathbb{O}_j$ using a type-f_l transceiver is represented by $r^\tau_{\mathbb{O}_i, \mathbb{O}^{f_l}_j}$. Given that satellite movement is both predictable and periodic, the propagation delay for the link $(\mathbb{O}_i, \mathbb{O}_j)$ can be determined and is denoted as $D^\tau_{(\mathbb{O}_i, \mathbb{O}_j)}$ (measured in milliseconds). The propagation delay is calculated by dividing the line-of-sight distance between nodes $\mathbb{O}_i$ and $\mathbb{O}_j$ by the light speed.

III. The LP-Based Optimal Multi-Path Heterogeneous-Transceiver Data Transmission Scheme

In this section, we explore the multi-path transmission of real-time remote sensing data using heterogeneous transceivers on time-varying graphs. We model the multi-path transmission constraints and transceiver matching constraints, followed by formulating the problem as a nonlinear programming model and transforming it into a linearized form.

A. Basic Constraints for Multi-Path Data Transmission

We define $x^\tau_{\mathbb{O}_i, \mathbb{O}_j} \geq 0$ as the achievable data rate through the link $(\mathbb{O}_i, \mathbb{O}_j) \in \mathcal{L}^\tau$ during time interval τ. Inherently, the

following constraints apply to data rate allocation.

1) Sending data rate constraints: Firstly, the allocated sending data rate for each transmission link must not exceed the maximum feasible transmission rate supported by the sender's available transceiver, which can be formulated as:

$$x^{\tau}_{\mathbb{O}_i,\mathbb{O}_j} \leq \max\{r^{\tau}_{\mathbb{O}_i^{f_l},\mathbb{O}_j} | w^{f_l}_{\mathbb{O}_i} = w^{f_l}_{\mathbb{O}_j} = 1, f_l \in \mathcal{F}\}. \quad (1)$$

2) Receiving data rate constraints: Likewise, the allocated sending data rate for each transmission link must not exceed the maximum feasible transmission rate supported by the receiver's available transceiver, which can be formulated as:

$$x^{\tau}_{\mathbb{O}_i,\mathbb{O}_j} \leq \max\{r^{\tau}_{\mathbb{O}_i,\mathbb{O}_j^{f_l}} | w^{f_l}_{\mathbb{O}_j} = w^{f_l}_{\mathbb{O}_i} = 1, f_l \in \mathcal{F}\}. \quad (2)$$

3) Flow conservation constraints: For every intermediate node except the source and destination UEs, it is necessary to ensure that incoming data rates match outgoing data rates to maintain real-time data transmission without accumulating data backlogs. Thus, $\forall \mathbb{O}_\xi \in \mathcal{V}^\tau - \{\mathbb{U}_s, \mathbb{U}_d\}$,

$$\sum_{\mathbb{O}_k:(\mathbb{O}_k,\mathbb{O}_\xi)\in\mathcal{L}^\tau} x^{\tau}_{\mathbb{O}_k,\mathbb{O}_\xi} = \sum_{\mathbb{O}_k:(\mathbb{O}_\xi,\mathbb{O}_k)\in\mathcal{L}^\tau} x^{\tau}_{\mathbb{O}_\xi,\mathbb{O}_k}. \quad (3)$$

4) Transceiver Matching Constraints: As previously stated, each type of transceiver can only establish communication with others of the same type within their reachable range. To ensure seamless transmission from the source UE to the sink UE, every link selected in the path must adhere to transceiver matching constraints. Specifically, for each link $(\mathbb{O}_i, \mathbb{O}_j) \in \mathcal{L}^\tau$, if $x^{\tau}_{\mathbb{O}_i,\mathbb{O}_j} > 0$, nodes at both ends of the link must utilize identical type of transceivers. This condition can be formally expressed as:

$$\exists w^{f_l}_{\mathbb{O}_i} = w^{f_l}_{\mathbb{O}_j} = 1, f_l \in \mathcal{F}, \text{ if } x^{\tau}_{\mathbb{O}_i,\mathbb{O}_j} > 0. \quad (4)$$

Constraint (4) indicates that a link $(\mathbb{O}_i, \mathbb{O}_j) \in \mathcal{L}^\tau$ can be selected as part of a path if and only if both nodes $\mathbb{O}_i$ and $\mathbb{O}_j$ have the same type of transceiver.

B. Linearizaion of Logical Constraints

Since equation (4) represents a logical constraint, it renders the routing problem non-linear in nature. Nevertheless, this constraint (4) can be transformed into an equivalent form expressed as:

$$x^{\tau}_{\mathbb{O}_i,\mathbb{O}_j} \leq M \cdot \sum_{f_l\in\mathcal{F}} w^{f_l}_{\mathbb{O}_i} \cdot w^{f_l}_{\mathbb{O}_j}, (\mathbb{O}_i, \mathbb{O}_j) \in \mathcal{L}^\tau, \quad (5)$$

where M is a large constant frequently employed in logical constraint reformulation. Here, M is designated as 10^9. Constraint (5) enforces $x^{\tau}_{\mathbb{O}_i,\mathbb{O}_j} > 0$ only when $\sum_{f_l\in\mathcal{F}} w^{f_l}_{\mathbb{O}_i} \cdot w^{f_l}_{\mathbb{O}_j} \geq 1$, indicating that nodes $\mathbb{O}_i$ and $\mathbb{O}_j$ must share at least one transceiver type. Therefore, constraint (4) is equivalently transformed into a linear form. Therefore, all the constraints of the routing problem are linear, enabling the problem to be solved using existing mathematical solvers.

C. Problem Formulation

The objective of the multi-path heterogeneous-transceiver transmission problem is to maximize the data rate from $\mathbb{U}_s$ to $\mathbb{U}_d$ within the specified time window τ. Thus, we formulate the problem as follows:

$$\begin{aligned}\mathbf{P1}: \max\ & R^\tau = \sum_{\mathbb{O}_k\in\mathcal{V}^\tau-\{\mathbb{O}_s\}} x^{\tau}_{\mathbb{U}_s,\mathbb{O}_k} = \sum_{\mathbb{O}_k\in\mathcal{V}^\tau-\{\mathbb{U}_d\}} x^{\tau}_{\mathbb{O}_k,\mathbb{U}_d}, \\ \text{s.t. } & (1)-(3), (5), \\ & x^{\tau}_{\mathbb{O}_i,\mathbb{O}_j} \geq 0.\end{aligned}$$

where the R^τ is the maximum achievable data rate from $\mathbb{U}_s$ to $\mathbb{U}_d$ during the given time interval τ. As both the objective function and the constraints are linear, the problem **P1** is formulated as a linear programming (LP) problem. Such problems can be optimally solved using mathematical optimization solvers like CVXPY [36], with a polynomial time complexity of $\mathcal{O}(|\mathcal{L}^\tau|^{3.5})$. However, for large-scale networks, this complexity remains high, limiting its applicability in real-time decision-making scenarios. Even for moderately sized instances of **P1**, the computation time may range from minutes to hours. For larger instances, it may extend to days. Therefore, efficient methods that exploit the specific structure of **P1** are necessary to address these scalability challenges.

IV. The Proposed Graph-Based Maximum-Flow Routing Algorithm

To address the complexity issues in large-scale satellite networks, we propose a graph theory-based method that utilizes traditional maximum flow calculations on a modified snapshot graph. This approach incorporates a carefully designed heterogeneous link resource representation rule. Specifically, we introduce auxiliary attributes in the snapshot graph to denote link availability. These attributes stem from the representation rule that converts node transceiver attributes into link availability attributes over the time-varying graph. By leveraging these attributes, we efficiently remove infeasible links, enabling the use of classical single-commodity maximum flow algorithms to solve the problem effectively.

A. Representation Rule of Heterogeneous Transceivers

Current single-commodity maximum flow algorithms do not account for the heterogeneous transceivers of nodes, making them unsuitable for directly addressing the formulated problem. To overcome this limitation, we enhance the snapshot graph by introducing additional link attributes. These attributes serve to translate the heterogeneous transceiver resources of nodes into properties associated with the links.

Firstly, we define the binary vector $\mathcal{Q}_{(\mathbb{O}_i,\mathbb{O}_j)} = \{q^{f_l}_{(\mathbb{O}_i,\mathbb{O}_j)} | f_l \in \mathcal{F}\}$ for each link $(\mathbb{O}_i, \mathbb{O}_j)$, where $q^{f_l}_{(\mathbb{O}_i,\mathbb{O}_j)} = 1$ means both node $\mathbb{O}_i$ and node $\mathbb{O}_i$ are equipped with transceivers of type f_l. The relationship can be expressed as:

$$\text{if } \exists w^{f_l}_{\mathbb{O}_i} = w^{f_l}_{\mathbb{O}_j}, f_l \in \mathcal{F}, f_l \in \mathcal{F}, \text{ then } q^{f_l}_{(\mathbb{O}_i,\mathbb{O}_j)} = 1. \quad (6)$$

Besides, to represent the link availability, we define the binary indicator $\tilde{q}_{(\mathbb{O}_i,\mathbb{O}_j)}$ for each link $(\mathbb{O}_i, \mathbb{O}_j)$, where $\tilde{q}_{(\mathbb{O}_i,\mathbb{O}_j)} = 1$ means node $\mathbb{O}_i$ can communicate with node $\mathbb{O}_j$. This relationship can be expressed as:

$$\text{if } \exists q^{f_l}_{(\mathbb{O}_i,\mathbb{O}_j)} = 1, f_l \in \mathcal{F}, \text{ then } \tilde{q}_{(\mathbb{O}_i,\mathbb{O}_j)} = 1. \quad (7)$$

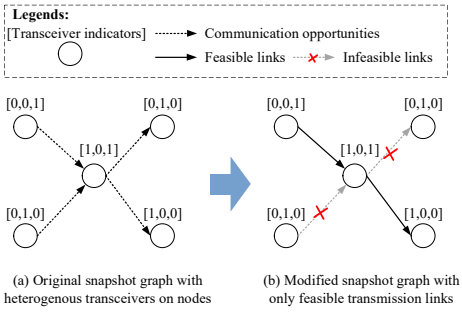

(a) Original snapshot graph with heterogenous transceivers on nodes

(b) Modified snapshot graph with only feasible transmission links

Fig. 2. Representation of heterogeneous transceiver resources over the time-varying graphs.

For ease of the illustration, we present an example of an satellite network with three types of transceivers (i.e., f_1, f_2, and f_3) in Figure 2. In Figure 2(a), there are five nodes and four potential communication opportunities. Each node has a transceiver indicator vector, such as $[1, 0, 1]$, indicating the node has transceivers of type-f_1 and type-f_3. The dashed arrows represent possible communication opportunities, meaning the nodes are within communication range. If the nodes connected by a dashed arrow have matched transceivers, the data can be transmitted between them. In Figure 2(b), after calculating the link availability attributes based on transceiver indicator vectors of different nodes, communication links without matching transceivers can be removed from the original snapshot graph to purify the solution space. As a result, the traditional single-source single-sink maximum flow algorithm can operate on the modified snapshot graph to find the optimal solution of **P1**.

By incorporating link availability attributes into the snapshot graph, the transceiver matching constraints for nodes in (5) are converted into on link attributes. Only links connecting a pair of nodes within communication range having the same transceivers are retained in the original network. For clarity, we present the step-by-step procedure in **Algorithm 1** outlining how heterogeneous transceiver resources are represented across the evolving graph structure.

B. The Graph-Based Optimal Heterogeneous-Transceiver Max-Flow Transmission Scheme and Complexity Analysis

With the representation rule in **Algorithm 1**, communication opportunities that are not feasible for data transmission due to the mismatch of transceivers are removed from the snapshot graph. Finally, **P1** can be optimally solved by running the single-commodity maximum flow algorithm over the modified graph $\mathcal{G}'^{\tau}$ after running **Algorithm 1**. Based on the proposed graph-based method, transforming transceiver resources into link attributes involves $O(|\mathcal{L}^{\tau}||\mathcal{F}|)$ computational operations. The time complexity of the state-of-the-art algorithm for solving single-commodity single-source single-sink maximum flow is $\mathcal{O}(|\mathcal{V}^{\tau}|^2|\mathcal{L}^{\tau}|)$. Therefore, the computational complexity of our proposed graph-based method, in the worst-case case, is $\mathcal{O}((|\mathcal{V}^{\tau}|^2 + |\mathcal{F}|)|\mathcal{L}^{\tau}|)$. This complexity indicates that the proposed method scales in a polynomial manner with the size of the network. In fact, since **Algorithm 1** can remove a large proportion of unfeasible links in $\mathcal{L}^{\tau}$, our method will have a shorter execution time than the theoretical one in most cases.

Algorithm 1 The representation rule of heterogeneous transceiver resources in the snapshot graph

Input: The original snapshot graph $\mathcal{G}^{\tau} = \{\mathcal{V}^{\tau}, \mathcal{L}^{\tau}\}$.

Output: The modified snapshot graph with the transformation of heterogeneous transceiver resources.

Define binary vector $\mathcal{Q}_{(\mathbb{O}_i,\mathbb{O}_j)} = \{q^{f_l}_{(\mathbb{O}_i,\mathbb{O}_j)} | f_l \in \mathcal{F}\}$ for each link $(\mathbb{O}_i, \mathbb{O}_j)$, where $q^{f_l}_{(\mathbb{O}_i,\mathbb{O}_j)} = 1$ means both of node $\mathbb{O}_i$ and node $\mathbb{O}_i$ has equipped with transceiver of type f_l. If $q^{f_l}_{(\mathbb{O}_i,\mathbb{O}_j)} = 0$, transceiver of type f_l is either unavailable on node $\mathbb{O}_i$ or node $\mathbb{O}_j$.
Define link availability indicator $\tilde{q}_{(\mathbb{O}_i,\mathbb{O}_j)}$ for each link $(\mathbb{O}_i, \mathbb{O}_j)$, where $\tilde{q}_{(\mathbb{O}_i,\mathbb{O}_j)} = 1$ means node $\mathbb{O}_i$ can communicate with node $\mathbb{O}_j$.
for each link $(\mathbb{O}_i, \mathbb{O}_j) \in \mathcal{L}^{\tau}$ **do**
    Initialize $\tilde{q}_{(\mathbb{O}_i,\mathbb{O}_j)} = 0$.
    for each transceiver type $f_l \in \mathcal{F}$ **do**
        if $w^{f_l}_{\mathbb{S}_i} = 1$ and $w^{f_l}_{\mathbb{S}_j} = 1$ **then**
            Set link attribute $q^{f_l}_{(\mathbb{O}_i,\mathbb{O}_j)} = 1$, $\tilde{q}_{(\mathbb{O}_i,\mathbb{O}_j)} = 1$.
        else
            Set link attribute $q^{f_l}_{(\mathbb{O}_i,\mathbb{O}_j)} = 0$.
    if $\tilde{q}_{(\mathbb{O}_i,\mathbb{O}_j)} = 0$ **do**
        Remove link $(\mathbb{O}_i, \mathbb{O}_j)$ from $\mathcal{L}^{\tau}$.
return The modified graph $\mathcal{G}'^{\tau}$.

V. Performance Evaluation

A. Simulation Setup

Our simulation involves a satellite network consisting of the Gaofen and Starlink constellations and four ground stations. Specifically, we choose 6 Gaofen satellites and 100-2,000 Starlink satellites from the object database of systems tool kit (STK) [37]. The four ground stations are positioned in the following coordinates: Beijing $(40°N, 116°E)$, Xi'an $(34.27°N, 108.93°E)$, Kashi $(39.5°N, 76°E)$, and Sanya $(18°N, 109.5°E)$. Each satellite is configured with two types of transceivers (i.e, RF and FSO) with an availability probability of 0.5 to mimic environmental distortions as in [12]. The communication opportunities between node pairs within the satellite network are determined using STK. ISLs and USLs equipped with RF transceivers operate at transmission rates uniformly selected from the range of $[300, 350]$ Mbps, while the maximum achievable transmission rate of FSO transceivers is set as 1.8 Gbps [15]. For both ISLs and USLs, the propagation delays are in the range of $[5, 15]$ ms as in [23].

To underscore the significance of the proposed approach, we assess the performance of the LP-based scheme (i.e., Combined RF/FSO-LP solver) and graph-based scheme (i.e., Combined RF/FSO-maxflow), as well as two baseline schemes using single-type of transceivers, i.e., *Pure RF scheme* and *Pure FSO scheme*. The *Pure RF-maxflow* scheme and *Pure FSO-maxflow* scheme use only one type of transceivers (i.e., either RF or FSO) and calculate the flow paths by running

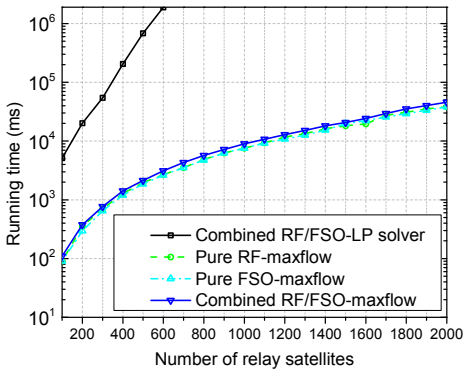

Fig. 3. Running times versus different network sizes.

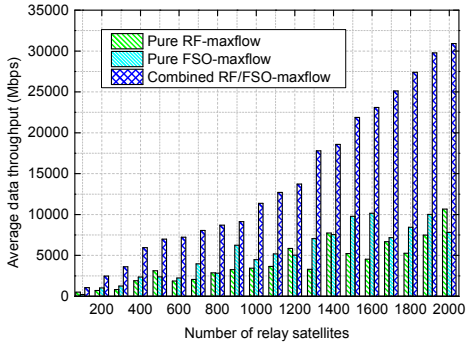

Fig. 4. Average throughput versus network sizes using different methods.

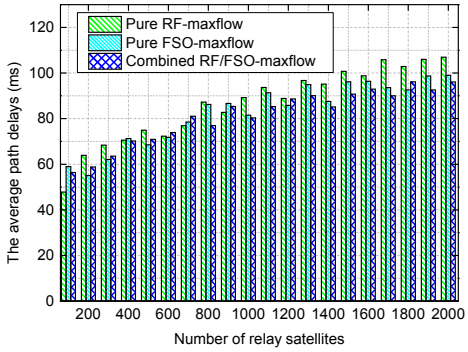

Fig. 5. Path delays versus network sizes under different methods.

one time of the Ford-Fulkerson maximum flow algorithm. The implementation of the algorithms is based on Python programming language, utilizing the functionalities offered by the NetworkX library.

B. Simulation Results and Analysis

Figure 3 displays the average running times of the four compared schemes while varying the number of LEO relay satellites from 100 to 2,000. With the increases of the number of relay satellites, the average running time of all the four schemes also increases. However, the graph-based methods exhibit significantly faster performance compared to the LP-based method. This can be attributed to the following reasons. For the LP-based scheme (i.e., Combined RF/FSO-LP solver), as the number of relay satellites increases, more communication opportunities are incorporated into the snapshot graph. This results in an escalation of decision variables and a nearly exponential rise in average running times. Since computational complexities of all the graph-based schemes are polynomial with network sizes, their average running times increase linearly as the number of relay satellites increases. As expected, the average running time of the Combined RF/FSO-maxflow scheme is slightly higher compared to those using single-type transceivers, indicating that the additional computational overhead introduced by the proposed algorithm is very small. Therefore, our proposed algorithm can support multi-path transmission in satellite networks with heterogeneous transceivers without significantly increasing complexity.

Figure 4 plots the average data throughput of the compared schemes with different relay satellite numbers. With more relay satellites, the average data throughput of all schemes tends to increase. This shows that the increase of relay satellite numbers can bring enhanced network connectivity to support higher data throughput for remote sensing data transmission applications. It is interesting that the average throughput of all the single-transceiver-based schemes are comparable with each other. This is expected because with pure RF or FSO links, feasible paths are limited as many links are unavailable with the movement of the satellites. In contrast, combined RF/FSO can achieve significant gains, even surpassing the sum of pure RF and pure FSO. This is because combined RF/FSO can exploit many additional communication opportunities. When RF is unavailable for the next hop, it can switch to an FSO link to construct the path, thus finding more feasible paths and greatly enhancing data transmission throughput.

Figure 5 depicts how the average path delay changes with varying numbers of relay satellites. As shown in Figure 5, the increase of relay satellite numbers will roughly cause an increase of average path delays for all the schemes. Under all system parameters, the average path delays of the algorithms are comparable with one another. This shows that the dominant factor affecting the delay is the relay satellite numbers and the density of satellites over space, since the larger satellite numbers can bring enhanced connectivity among satellites.

VI. Conclusion

In the realm of large-scale satellite networks and the deployment of heterogeneous ISL technologies aimed at transmitting real-time data with low latency and high throughput globally, this study investigates whether heterogeneous ISL s and multi-path transmission can enhance real-time remote sensing data transmission throughput. Specifically, we explore a multi-path routing strategy tailored for real-time remote sensing applications. We recognize that formulating this routing problem as an LP problem introduces high computational complexities when using mathematical solvers. To tackle this issue, we develop a graph-based scheme that facilitates the adaptation of single-commodity maximum flow algorithms to efficiently achieve optimal solutions within polynomial time. Simulations conducted on the Gaofen and Starlink constellations demonstrate

a significant increase in data throughput compared to those utilizing single-type transceivers.

VII. Acknowledgement

This research is supported by the National Research Foundation, Singapore, and Infocomm Media Development Authority under its Future Communications Research & Development Programme, Defence Science Organisation (DSO) National Laboratories under the AI Singapore Programme (AISG Award No: AISG2-RP-2020-019 and FCP-ASTAR-TG-2022-003), and Singapore Ministry of Education (MOE) Tier 1 (RG87/22). This work of B. Guo is supported by the Fundamental Research Funds for the Central Universities and the Innovation Fund of Xidian University under Grant YJSJ23012 and YJSJ24017, and in part by the Fund of China Scholarship Council (CSC). The work of Z. Han is supported by NSF CNS-2107216, CNS-2128368, CMMI-2222810, ECCS-2302469, US Department of Transportation, Toyota. Amazon and Japan Science and Technology Agency (JST) Adopting Sustainable Partnerships for Innovative Research Ecosystem (ASPIRE) JPMJAP2326. This work was done when B. Guo was a visiting student at SUTD sponsored by the CSC. The corresponding author is Z. Xiong.

References

[1] J. Choi, "Enhancing reliability in leo satellite networks via high-speed inter-satellite links," *IEEE Wireless Commun. Letters*, May 2024.

[2] B. Al Homssi, A. Al-Hourani, K. Wang, P. Conder, S. Kandeepan, J. Choi, B. Allen, and B. Moores, "Next generation mega satellite networks for access equality: Opportunities, challenges, and performance," *IEEE Commun. Mag.*, vol. 60, no. 4, pp. 18–24, Apr. 2022.

[3] D. Yang, J. Yang, G. Li, Y. Zhou, and C. Tang, "Globalization highlight: orbit determination using BeiDou inter-satellite ranging measurements," *GPS Solut.*, vol. 21, no. 3, pp. 1395–1404, Apr. 2017.

[4] Aerospace-technology, "Iridium next satellite constellation," https://www.aerospace-technology.com/projects/iridium-next-satellite-constellation/.

[5] SPACEFLIGHT-NOW, "Spacex passes 2,500 satellites launched for starlink internet network," https://spaceflightnow.com/2022/05/13/spacex-passes-2500-satellites-launched-for-companys-starlink-network/, 2022.

[6] "Chinas new space race: First satellite of cascs Hongyan leo satcom constellation to launch by end of 2018," https://spacewatch.global/.

[7] Z. Lai, W. Liu, Q. Wu, H. Li, J. Xu, and J. Wu, "SpaceRTC: Unleashing the low-latency potential of mega-constellations for real-time communications," in *Proc. IEEE Conf. on Comput. Commun. (INFOCOM)*, London, UK, Jun. 2022, pp. 1339–1348.

[8] H. Ramapriyan, "The role and evolution of nasa's earth science data systems," in *IEEE EDS/CAS Chapter Meeting*, no. GSFC-E-DAA-TN24713, CA, Aug. 2015.

[9] V. C. Gomes, G. R. Queiroz, and K. R. Ferreira, "An overview of platforms for big earth observation data management and analysis," *Remote Sensing*, vol. 12, no. 8, pp. 1253–1277, Apr. 2020.

[10] P. Soille, A. Burger, D. De Marchi, P. Kempeneers, D. Rodriguez, V. Syrris, and V. Vasilev, "A versatile data-intensive computing platform for information retrieval from big geospatial data," *Future Generation Computer Systems*, vol. 81, pp. 30–40, Apr. 2018.

[11] G. Araniti, N. Bezirgiannidis, E. Birrane, I. Bisio, S. Burleigh, C. Caini, M. Feldmann, M. Marchese, J. Segui, and K. Suzuki, "Contact graph routing in DTN space networks: overview, enhancements and performance," *IEEE Commun. Mag.*, vol. 53, no. 3, pp. 38–46, Mar. 2015.

[12] B. Guo, Z. Chang, Z. Han, W. Yang, and Z. Xiong, "Network slicing strategy for real-time applications in large-scale satellite networks with heterogeneous transceivers," *IEEE Wireless Commun. Lett.*, May 2024.

[13] Q. Chen, L. Yang, Y. Zhao, Y. Wang, H. Zhou, and X. Chen, "Shortest path in LEO satellite constellation networks: An explicit analytic approach," *IEEE J. Sel. Areas in Commun.*, vol. 42, no. 5, pp. 1175–1187, Feb. 2024.

[14] NASA, "State of the art of small spacecraft technology," https://www.nasa.gov/.

[15] H. Zech, F. Heine, D. Tröndle, S. Seel, M. Motzigemba, R. Meyer, and S. Philipp-May, "LCT for EDRS: LEO to GEO optical communications at 1, 8 Gbps between Alphasat and Sentinel 1a," in *Unmanned/Unattended Sensors and Sensor Networks XI; and Advanced Free-Space Optical Communication Techniques and Applications*, vol. 9647. SPIE, Oct. 2015, pp. 85–92.

[16] S. Aggarwal, S. K. Saha, I. Khan, R. Pathak, D. Koutsonikolas, and J. Widmer, "Musher: An agile multipath-tcp scheduler for dual-band 802.11 ad/ac wireless lans," *IEEE/ACM Trans. Netw.*, vol. 30, no. 4, pp. 1879–1894, Mar. 2022.

[17] F. Tang, H. Zhang, and L. T. Yang, "Multipath cooperative routing with efficient acknowledgement for LEO satellite networks," *IEEE Trans. Mobile Computing*, vol. 18, no. 1, pp. 179–192, Apr. 2018.

[18] K. Sakai, M.-T. Sun, and W.-S. Ku, "Data-intensive routing in delay-tolerant networks," in *IEEE INFOCOM 2019*, Paris, France, Apr. 2019, pp. 2440–2448.

[19] P. Wang, H. Li, B. Chen, and S. Zhang, "Enhancing earth observation throughput using inter-satellite communication," *IEEE Trans. Wireless Commun.*, vol. 21, no. 10, pp. 7990–8006, Apr. 2022.

[20] F. Tang, "Dynamically adaptive cooperation transmission among satellite-ground integrated networks," in *IEEE INFOCOM 2020*, Toronto, Canada, Jul. 2020, pp. 1559–1568.

[21] L. Chen, F. Tang, X. Li, J. Liu, Y. Yang, J. Yu, and Y. Zhu, "Delay-optimal cooperation transmission in remote sensing satellite networks," *IEEE Trans. Mobile Computing*, vol. 22, no. 9, pp. 5109–5123, May 2023.

[22] H. F. Salama, D. S. Reeves, and Y. Viniotis, "A distributed algorithm for delay-constrained unicast routing," in *IEEE Proceedings of INFOCOM*, vol. 1, Kobe, Japan, Apr. 1997, pp. 84–91.

[23] B. Guo, H. Li, Z. Zhang, and Y. Yan, "Online network slicing for real time applications in large-scale satellite networks," in *IEEE Int. Conf. Commun.*, Rome, Italy, Jun. 2023, pp. 5564–5569.

[24] E. Ekici, I. F. Akyildiz, and M. D. Bender, "A distributed routing algorithm for datagram traffic in LEO satellite networks," *IEEE/ACM Trans. Networking*, vol. 9, no. 2, pp. 137–147, Apr. 2001.

[25] B. Guo, Z. Xiong, B. Wang, T. Q. S. Quek, and Z. Han, "Semantic communication-aware end-to-end routing in large-scale LEO satellite networks," in *IEEE MetaCom*, Hongkong, Aug. 2024.

[26] P. Wang, X. Zhang, S. Zhang, H. Li, and T. Zhang, "Time-expanded graph-based resource allocation over the satellite networks," *IEEE Wireless Commun. Lett.*, vol. 8, no. 2, pp. 360–363, Sep. 2018.

[27] W. Ding, B. Guo, and Z. Xiong, "Virtualized computing and communication service provision in large-scale software defined satellite networks," in *IEEE/CIC Int. Conf. Commun. China (ICCC)*, Hangzhou, China, Aug. 2024.

[28] M. Sheng, Y. Wang, J. Li, R. Liu, D. Zhou, and L. He, "Toward a flexible and reconfigurable broadband satellite network: Resource management architecture and strategies," *IEEE Wireless Commun.*, vol. 24, no. 4, pp. 127–133, Jun. 2017.

[29] Y. Wang, M. Sheng, W. Zhuang, S. Zhang, N. Zhang, R. Liu, and J. Li, "Multi-resource coordinate scheduling for earth observation in space information networks," *IEEE J. Selected Areas Commun.*, vol. 36, no. 2, pp. 268–279, Feb. 2018.

[30] D. Zhou, M. Sheng, X. Wang, C. Xu, R. Liu, and J. Li, "Mission aware contact plan design in resource-limited small satellite networks," *IEEE Trans. Commun.*, vol. 65, no. 6, pp. 2451–2466, Mar. 2017.

[31] D. Zhou, M. Sheng, R. Liu, Y. Wang, and J. Li, "Channel-aware mission scheduling in broadband data relay satellite networks," *IEEE J. Selected Areas in Commun.*, vol. 36, no. 5, pp. 1052–1064, May 2018.

[32] V. V. Gounder, R. Prakash, and H. Abu-Amara, "Routing in LEO-based satellite networks," in *IEEE Emerging Tech. Symposium Wireless Commun. and Systems*, Richardson, TX, Apr. 1999, pp. 22.1–22.6.

[33] M. Werner, "A dynamic routing concept for ATM-based satellite personal communication networks," *IEEE J. Sel. Areas Commun.*, vol. 15, no. 8, pp. 1636–1648, Oct. 1997.

[34] J. V. Evans, "Satellite systems for personal communications," *Proc. the IEEE*, vol. 86, no. 7, pp. 1325–1341, Jun. 1998.

[35] Y. Hu, B. Guo, C. Yang, and Z. Han, "Time-deterministic networking for satellite-based internet-of-things services: Architecture, key technologies, and future directions," *IEEE Netw.*, Mar. 2024.

[36] S. Diamond and S. Boyd, "CVXPY: A Python-embedded modeling language for convex optimization," *The J. Machine Learning Research*, vol. 17, no. 1, pp. 2909–2913, Jan. 2016.

[37] A. A. Company, "Systems tool kit (STK)," https://www.agi.com/products/stk.